Trapping of plasma enabled by pycnoclinic acoustic force

John P. Koulakis,[1,*] Seth Pree,[1] Alexander L. F. Thornton,[2] and Seth Putterman[1]
[1]*Department of Physics and Astronomy, University of California, Los Angeles, Los Angeles, California 90095, USA*
[2]*Department of Electrical and Computer Engineering, University of Wisconsin, Madison, Madison, Wisconsin 53706, USA*

(Received 21 May 2018; revised manuscript received 21 July 2018; published 12 October 2018)

Sound can hold partially ionized sulfur at the center of a spherical bulb. We use the sulfur plasma itself to drive a 180 dB re 20 μPa sound wave by periodically heating it with microwave pulses at a frequency that matches the lowest order, spherically symmetric, acoustic resonance of the bulb. To clarify the trapping mechanism, we generalize acoustic radiation pressure theory to include gaseous inhomogeneities and find an interaction of high-amplitude sound with density gradients in the gas through which it propagates. This is the pycnoclinic acoustic force (PAF). Though generated by rapidly oscillating sound waves, it has a finite time average and manipulates the plasma through density gradients at its boundary. The PAF is essential for the description of the trap holding a plasma against its own buoyancy as well as understanding convection in the region outside the plasma. It has implications for pulse tubes, thermoacoustic engines, thermal vibrational convection in microgravity, combustion in the presence of sound, and the modeling of Cepheid variable stars.

DOI: 10.1103/PhysRevE.98.043103

I. INTRODUCTION

A sound field scattering off an object imparts momentum. This property, known as acoustic radiation pressure [1–6], has been exploited to design acoustical tweezers which can levitate metal in air [7] or hold bubbles in water [8]. In this paper we report experimental observations that a similar but more general acoustic effect can impart a spherically symmetric central force on the temperature gradient surrounding partially ionized sulfur gas in the center of a 3 cm bulb [Fig. 1(a)]. In the absence of the sound, the plasma expands to fill the bulb and floats to the top [Fig. 1(b)]. We describe how this capability arises theoretically by generalizing acoustic radiation pressure to include interactions between sound and density gradients in the ambient gas through which it propagates. A pycnoclinic acoustic force (PAF)—a time-averaged pressure on density gradients in the presence of a sound field—arises that is essential for understanding both the nature of the spherically symmetric force holding the plasma and the generation of periodic instabilities observed.

Sulfur plasma lamps form conditions conducive for observing the PAF for two reasons. First, the temperature changes from ∼4000 K at the center of the bulb to ∼1000 K near the glass, resulting in large density gradients at constant pressure. Second, partially ionized gases are fantastic acoustic transducers. They provide a unique method of sound transduction, whereby volumetric absorption of modulated rf (microwave) energy generates pressure waves directly in the gas [10–12].

II. APPARATUS

Our experimental setup uses a standard sulfur plasma lamp that is well described in the literature [13,14]. Microwaves from a conventional magnetron heat the sulfur to a final molecular density of $\sim 2\times10^{19}$ cm^{-3} and $\sim10^{-5}$ ionization fraction [15,16]. To drive acoustic resonances within the bulb, our magnetron power supply has been modified to be able to pulse at frequencies between 5 and 100 kHz, and 5–95% duty cycle, according to a design by Gavin *et al.* [17,18]. We have described our waveguide circuit elsewhere [19].

One challenge that is often encountered with plasma bulbs is that they are prone to sudden extinction. As the bulb heats up, the plasma inside begins to flicker randomly and violently until it spontaneously puts itself out. Reignition cannot occur until the bulb has cooled. We were able to completely suppress this behavior by spinning the bulb at a rate of about 50 Hz, an approach used in industry [14,20]. The rotation [21] reduces azimuthal asymmetry and provides a small centrifugal force to pull the plasma toward the axis. This is our normal state, seen in Fig. 1(b) and Supplemental video S1 [9].

In our system, the microwave power is always pulsed, but in the normal state the pulse frequency does not match any acoustic resonance. In the normal mode, the light output measured by a photodiode has a sawtooth-shaped ac component seen in Fig. 1(d). During the microwave pulse, the plasma heats and the light signal ramps up. Between pulses, the plasma cools and the light signal ramps down. When the pulse frequency matches a resonance, the plasma may confine itself to the central region of the bulb, as observed by Courret *et al.* [18] for time periods less than 1 s in a system that is not spinning. There is also a qualitative change in the photodiode signal [18]: in going from the normal to the trapped state, the ac component becomes sinusoidal instead of sawtooth [Fig. 1(c)]. We find that by simultaneously spinning the bulb, we are able to capture the plasma reproducibly and keep it confined indefinitely, a practical necessity to study the mechanism of action in detail. Videos of the trapped state (S2) and the transition to the trapped state (S3) can be found in the Supplemental Material [9].

*koulakis@physics.ucla.edu

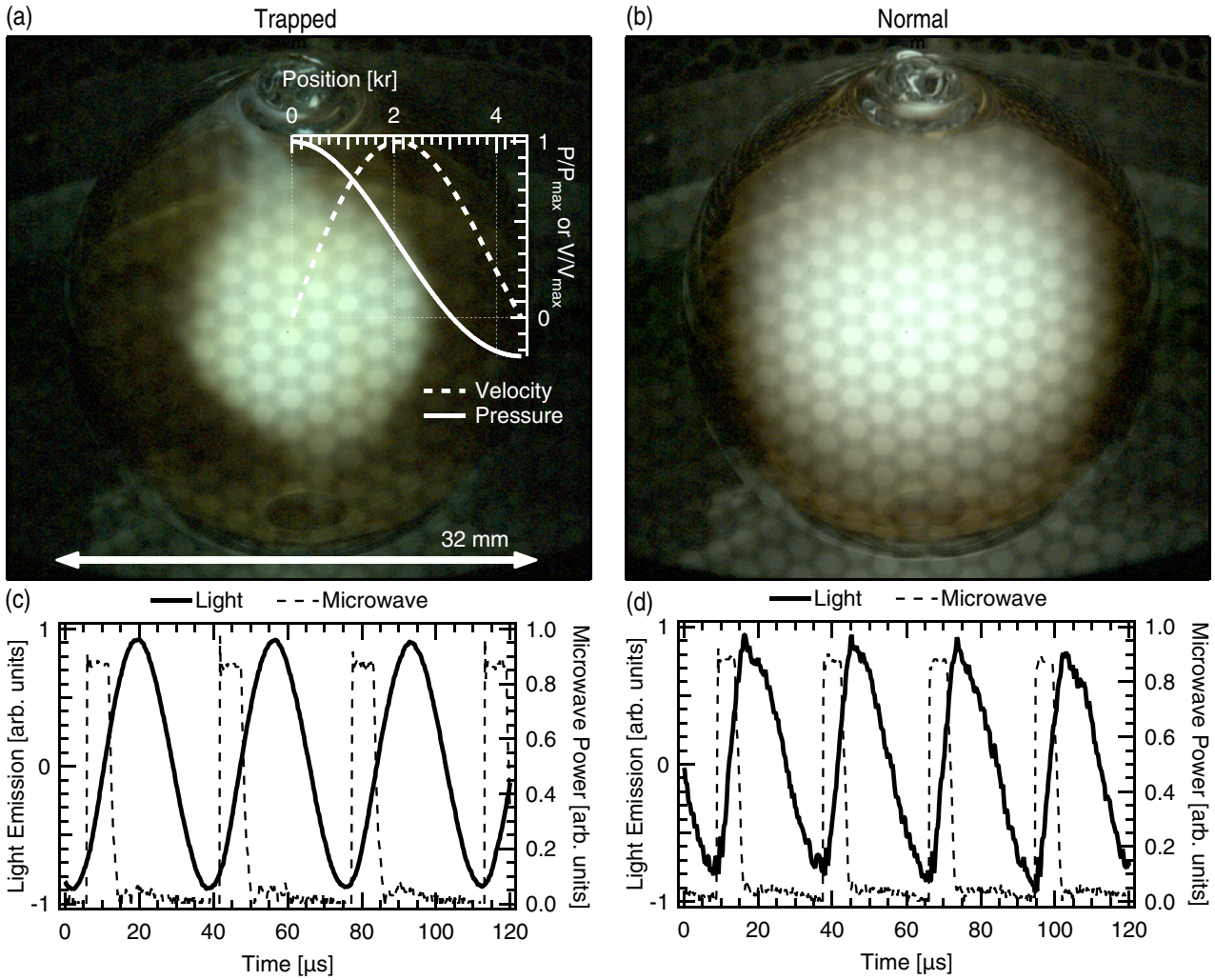

FIG. 1. (a) Pycnoclinic acoustic force holds plasma centrally in a spherical bulb. (b) In the absence of sound, the plasma fills the bulb. The bulb rotates at 50 Hz in both states; otherwise the bulb is prone to sudden extinction. Hexagonal shading in the images is due to the metallic mesh cavity surrounding the bulb. The light emission in the trapped (c) and normal (d) states is qualitatively different. The high-pass filtered signal transitions from sawtooth to sinusoidal in shape near an acoustic resonance. When the plasma is trapped, the peak-to-peak oscillation amplitude is 20× to 60× larger than in the normal state. Acoustic pressure and velocity in the lowest frequency, spherically symmetric mode are plotted in the inset of (a). High-speed videos of each state as well as of the transition from the normal to the trapped state are available in the Supplemental Material [9].

III. ACOUSTICS

To hold the plasma centrally in the bulb, as in Fig. 1(a), we appeal to the PAF generated by the first spherically symmetric acoustic "breather" mode. The persistence of light oscillations after the microwave is turned off gives the acoustic quality factor $Q = 700$–900, ascribed to the thermal boundary layer at the glass [22]. In a homogeneous medium, the acoustic pressure and velocity in this mode are given by the spherical Bessel functions,

$$P_1(r,t) = p_{\max}\frac{\sin kr}{kr}\, e^{i\omega t}, \tag{1}$$

$$\vec{v}_1(r,t) = -2.29\, v_{\max}\frac{\sin kr - kr\cos kr}{k^2r^2}\, i e^{i\omega t}\hat{r}, \tag{2}$$

which are plotted in the inset of Fig. 1(a). Here, $k = 4.49/R = \omega/c$, $R = 16$ mm is the radius of the bulb, c is the speed of sound, $p_{\max} = 2.29\,\rho_0 c\, v_{\max}$, and ρ_0 is the ambient density. The resonant frequency is $\omega/2\pi \approx 29$ kHz. Since the gas in our bulb is not homogeneous, we do not expect these functions to hold strictly. The general shape and properties of the mode, however, do not change in a way that substantially affects our subsequent arguments, and so we proceed using these functions as an approximation. The main effect of a hotter core is to shift the location of the velocity antinode toward the glass [23].

The sound amplitudes on resonance can be extremely high, exceeding 180 dB re 20 μPa. With a Vision Research Phantom v2512 high-speed camera capable of operating at 170 000 frames per second, we can observe the plasma size

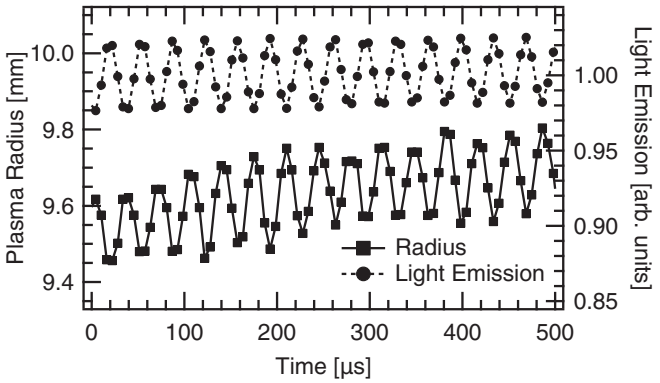

FIG. 2. Plasma size and spatially integrated light emission over time.

and light emission oscillations occurring within an acoustic period (see Supplemental video S4 [9]), and thereby measure the acoustic oscillation amplitude. The plasma radius and spatially integrated light emission over time are extracted to produce Fig. 2. We find that the radius and light oscillations are out of phase. This fact is the basis of our interpretation of the radial oscillations as a lower bound of the acoustic oscillation amplitude.

In the absence of acoustics, we expect oscillations in the plasma radius and light emission to be in phase because the luminous plasma volume grows when heated and shrinks when left alone. Without microwave pulses, but with a standing sound wave, the gas is heated during the acoustic compression and cooled during rarefaction. Since light emission increases with temperature, we expect light emission to be out of phase with the radial oscillations. Our observation that the curves are almost exactly out of phase demonstrates that heating due to acoustic compression is much larger than heating due to individual microwave pulses. In fact, oscillations of the luminous radius give only a lower bound of the acoustic oscillation amplitude, because compressive heating of gas near the light emission threshold partially offsets the inward acoustic motion. Figure 2 gives the oscillation amplitude as at least 0.1 mm, corresponding to $v_{\max} = 2\pi \times 0.1\ \text{mm} \times 30\ \text{kHz} = 18.8\ \text{m s}^{-1}$, Mach number of 0.03, and 180 dB sound level. We have seen $v_{\max}$ as high as $30\ \text{m s}^{-1}$.

IV. TIME-AVERAGED DYNAMICS

The PAF can be understood by an appropriate treatment of the fluid equations. Our derivation, which can be found in detail in Ref. [24], parallels that of the thermal vibrational convective force in Ref. [25], but with the major change that the "vibrational" fields are acoustic in our case, whereas they are incompressible in Ref. [25]. Another difference is that the theory in Ref. [25] is in the Boussinesq limit, whereas our derivation allows large temperature and density changes in the ambient fluid. See [26] for an analogous theory specialized to the field of microfluidics.

The fluid variables are separated by timescale into rapidly oscillating parts (sound) and slowly varying parts (response of background fluid). Keeping terms that are second order in the sound amplitude and time averaging over many acoustic periods leads to an Euler-like equation for the averaged velocity $\bar{v}$,

$$\bar{\rho}\,\frac{\partial \bar{v}}{\partial t} = -\nabla \bar{P} + \frac{\nabla\langle P_1^2\rangle}{2\bar{\rho}c^2} - \frac{\bar{\rho}}{2}\nabla\langle v_1^2\rangle - \langle v_1^2\rangle\nabla\bar{\rho} + \frac{\partial}{\partial t}\left\langle \frac{P_1\vec{v}_1}{c^2} - \rho_1\vec{v}_1 \right\rangle, \tag{3}$$

where $\bar{\rho}$ and $\bar{P}$ are the time-averaged but spatially varying background density and pressure and $\langle\cdot\rangle$ denotes time averaging over several acoustic periods. The rapidly oscillating sound pressure and velocity, P_1 and $\vec{v}_1$, are found to obey the wave equation for sound in an inhomogeneous medium [27,28], and are given approximately by Eqs. (1) and (2) in our case.

In the absence of sound and gravity, the inhomogeneous system sits at constant pressure and there is no flow. Turning the sound on leads to a flow in the background gas until an opposing pressure is built up (if possible). The time derivative term is zero in steady state, but also insignificant in the approach to steady state [24]. The second and third terms on the right-hand side of Eq. (3) are the well-known second-order pressure due to a sound field in a homogenous medium [2,6]. The fourth term acts on density gradients and thereby distinguishes the interface between hot and cold. It provides a handle to grab the plasma by its boundary and is the PAF responsible for trapping the plasma at the center of the bulb. Note that the length scale of the acoustic field gradients in the second and third terms is limited by the wavelength, whereas that of the density gradient is not. This allows the magnitude of the pycnoclinic term to be larger than the rest under certain circumstances and, in particular, ours. Since the temperature is monotonically decreasing from the center of our bulb outward, $\nabla\bar{\rho}$ is positive and there is an inward force acting on the plasma, holding it centered in the bulb and slightly compressing it by about 1%.

In our analysis leading to Eq. (3), we have ignored both the rotation [29] of the bulb and gravity. This is justified by considering that the gravitational force is small compared to the centripetal force, which in turn is small compared to the radiation pressure terms. The Coriolis force is suppressed by time averaging over the sound period, noting that $\Omega/\omega \ll 1$. Trapping requires that

$$\zeta = \frac{\langle v_1^2\rangle\nabla\bar{\rho}}{\bar{\rho}g} \gg \frac{\Omega^2 R}{g} > 1, \tag{4}$$

where Ω is the rotation frequency and g is the acceleration of gravity. For $\Omega/2\pi \approx 50$ Hz, we have $\Omega^2 R/g \sim 150$, and for $v \sim 20\ \text{m s}^{-1}$ and $\nabla\bar{\rho}/\bar{\rho} \sim 1/R$, $\zeta > 10^3$. Although we do not believe that the rotation is strictly necessary for trapping, we have found it is a practical necessity to achieve starting conditions with sufficient quiescence and symmetry to enter the trapped state.

V. CONVECTIVE INSTABILITY

The PAF also affects convective and thermal transport, demonstrated by periodic ejections of hot material from the plasma core, as seen in Fig. 3(a) and Supplemental video S5 [9]. These ejections keep the plasma radius within a narrow

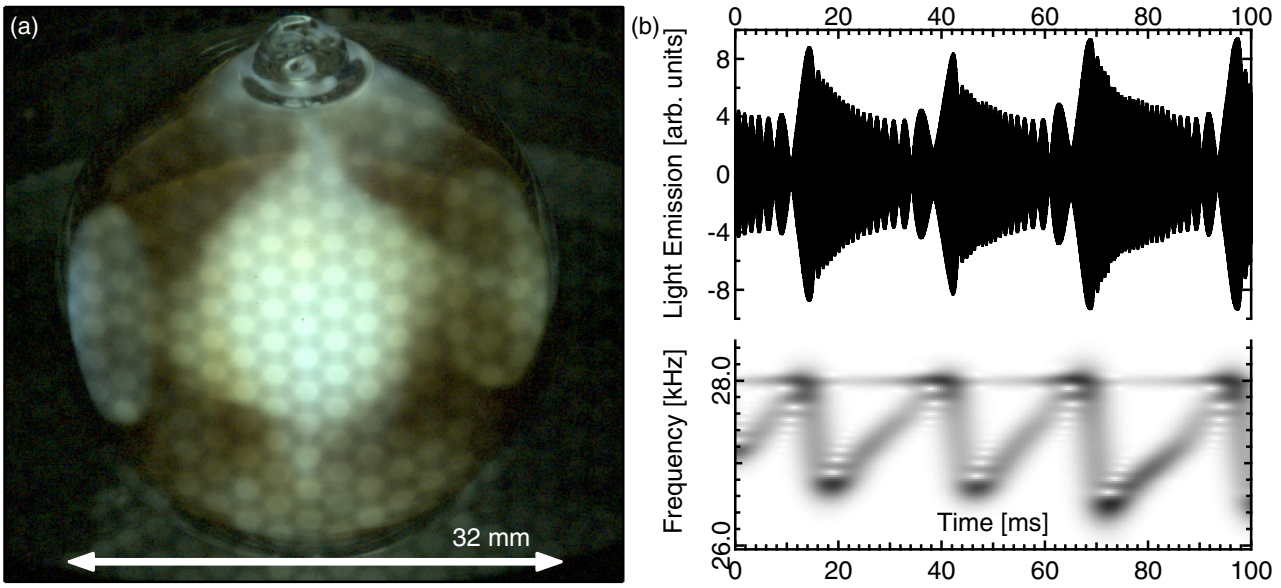

FIG. 3. Instability periodically generates ejections of warm material from the hot core (a) (shown in Supplemental video S5 [9]). The ejections cool when they reach the glass, lowering the acoustic resonant frequency. Beating between the drive frequency and frequency-shifted sound is seen in the high-pass filtered photodiode signal (b). Microwave heating slowly increases the gas temperature, and when the resonant frequency matches the drive, the sound amplitude rapidly builds up, driving the next ejection.

range of about $R/2$. They emanate from the central plasma until they reach the glass and turn back forming a mushroom-like shape. This advective heat transport to the glass is a rapid cooling event that lowers the bulb resonant frequency, detuning it from the drive. The sound field in the bulb is shifted in frequency, and decays over a timescale determined by the acoustic Q. We see the shifted frequency beating with the drive frequency in the high-pass filtered photodiode signal in Fig. 3(b). The sonogram [also in Fig. 3(b)] reveals a steady peak at the drive frequency of 28 kHz and a second, moving peak that slowly increases in frequency until it matches the drive, upon which it jumps by about -1 kHz. This process repeats with a periodicity of about 25 ms.

Stability considerations give insight into the mechanism driving the ejections and highlight the essential role of the PAF in confining the plasma. If $\langle v_1^2 \rangle$ and $\bar{\rho}$ are perfectly spherically symmetric, the right-hand side of Eq. (3) is irrotational and pressure can balance the acoustic forces to achieve equilibrium. When perturbations to spherical symmetry develop, the right-hand side of Eq. (3) has a nonzero solenoidal component, which can generate a circulating mass flow (the inception of the ejections). Taking the curl of both sides of Eq. (3) shows that the circulating flow obeys

$$\frac{\partial}{\partial t}\nabla\times(\bar{\rho}\bar{v}) = \frac{1}{2}\nabla\bar{\rho}\times\nabla\langle v_1^2\rangle. \tag{5}$$

Considering the sign of the circulation generated near perturbations when $\nabla\bar{\rho}$ is mainly in the $+\hat{r}$ direction shows that the circulating flow restores spherical symmetry when $\nabla\langle v_1^2\rangle\cdot\hat{r}>0$ and amplifies perturbations when $\nabla\langle v_1^2\rangle\cdot\hat{r}<0$. This is the cause of the stable spherical configuration in the region interior to the location of the velocity antinode, while periodic instability characterizes the region external to the location of the velocity antinode. Note that if the pycnoclinic acoustic force was not included in Eq. (3), the magnitude of the generated vorticity would be the same, but the sign would be opposite, resulting in stability criteria opposite to those observed.

The periodic ejections dramatically increase the averaged heat flow to the glass compared to the normal state. Figure 4 plots the glass temperature over time as it goes from the normal to the trapped state and back as measured by an FLIR-T400/HT ThermaCAM infrared camera [30]. When the plasma is trapped, the bulb temperature rises by 100 K. At these temperatures, the infrared gray body radiation emanating from the quartz itself is substantial, and a 100 K increase in bulb temperature corresponds to an additional $\sim$200 W of infrared gray body radiation. The microwave power absorbed by the plasma does not change by more than 1% when it goes into resonance. Evidently the increased glass

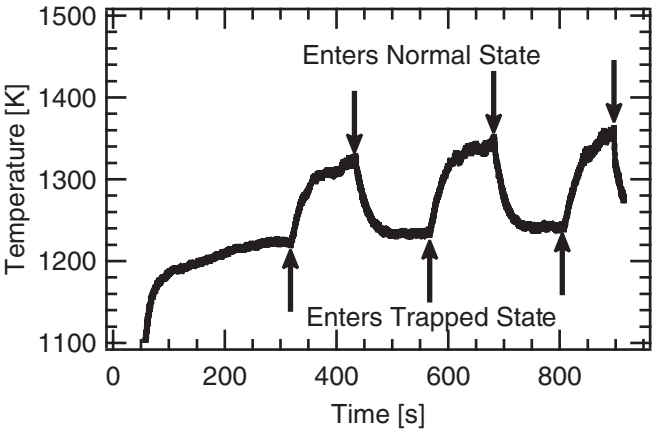

FIG. 4. Periodic ejections in the trapped state increase the heat flow to the quartz bulb, raising its temperature by $\sim$100 K.

heating comes at a cost of visible light emission, which is cut in half (data not shown).

VI. CONCLUSIONS

The PAF is important when a high-amplitude sound wave propagates in the presence of a large gradient in the background density. This gradient is maintained by external sources even when the sound field is weak. High-amplitude sound and large density gradients can be found in Rijke and Sondhauss tubes [31,32], the pinching of flames in combustion cylinders [33,34], and the mixing of different density gases, where Tuckermann [35] observed that the dense gas gets pulled into velocity antinodes of a standing wave. We propose that the second-order term studied here will play a role in a detailed theory of the Sondhauss tube, and in the other experiments this term will be important at leading order. The theory of thermal vibrational convection [25] has been used to gain insight into pulse tubes [36], particularly into the ability of vibration to suppress convection [37]. That theory [25] does lead to a time-averaged effect proportional to the imposed density gradient and the square of the fast vibration. However, it is carried out in the Boussinesq (i.e., incompressible) approximation and the second-order term vanishes when the thermal gradient is parallel to the direction of vibration. In this paper, the fluid is highly compressible and a time-averaged second-order term emerges even when the density gradient is parallel to the direction of vibration. A full understanding of the PAF will lead to devices incorporating geometries where sound and a density gradient generate a flow so as to make a gas pump without moving parts which operates in extreme conditions. Convection in microgravity, for example, can be controlled with acoustic fields. Analogous acoustic forces have been used in microfluidics to manipulate the interface between regions of varying salinity and sort small particles and/or cells [26,38,39].

We propose that the PAF also affects certain natural phenomena. For instance the Mach number for the radial pulsations of a classical Cepheid variable star is comparable to the Mach number observed in this work. These stars are important for benchmarking extragalactic distances. Comparing the size of the PAF and traditional acoustic radiation pressure to the gravitational force in these stars shows that the acoustic effects are non-negligible and produce a time-averaged body force that should be considered in addition to gravity. Both traditional acoustic radiation pressure and the PAF scale as $v_{\max}^2\bar{\rho}/R$, where $v_{\max}$ is the star surface oscillation velocity, $\bar{\rho}$ is the star average density, and R is the star's radius. In the case of the PAF, we have conservatively taken the length scale of the density gradient to be R, but it is often much smaller [40–42]. By Newton's law, the gravitational force at the surface of the star is $GM\bar{\rho}/R^2$, with G being the gravitational constant and M the mass of the star. The ratio of the two give a unitless parameter $v_{\max}^2 R/GM$ describing the role of acoustic forces. With typical parameters for a classical Cepheid ($M = 13M_\odot$, $R = 169R_\odot$, $v_{\max} = 20\,000\ \mathrm{m\,s^{-1}}$ for ℓ Carinae [43–45]), this parameter is 0.03, meaning acoustic forces are about 3% those of gravity. The PAF becomes a leading-order effect when the density gradient occurs over a distance of a few percent of the star's radius, and could alter its internal structure.

ACKNOWLEDGMENTS

We thank Vision Research for a demonstration of their Phantom v2512 high-speed camera, which resulted in some of the data presented here. We thank Gilles Courret for demonstrating acoustic confinement in plasma lamps and introducing us to this topic, and Greg Swift, Pat Diamond, Jonathan Aurnou, and Alex Bataller for illuminating discussions. This material is based upon work supported by the Air Force Office of Scientific Research under Award No. FA9550-16-1-0271. Initial stages of this project were funded by the DARPA MTO.

[1] L. V. King, On the acoustic radiation pressure on spheres, Proc. R. Soc. A **147**, 212 (1934).
[2] L. P. Gor'kov, On the forces acting on a small particle in an acoustical field in an ideal fluid, Sov. Phys. Doklady **6**, 773 (1962).
[3] M. Barmatz and P. Collas, Acoustic radiation potential on a sphere in plane, cylindrical, and spherical standing wave fields, J. Acoust. Soc. Am. **77**, 928 (1998).
[4] S. Putterman, J. Rudnick, and M. Barmatz, Acoustic levitation and the Boltzmann-Ehrenfest principle, J. Acoust. Soc. Am. **85**, 68 (1998).
[5] R. Löfstedt and S. Putterman, Theory of long wavelength acoustic radiation pressure, J. Acoust. Soc. Am. **90**, 2027 (1998).
[6] T. G. Wang and C. P. Lee, Radiation pressure and acoustic levitation, in *Nonlinear Acoustics*, edited by M. F. Hamilton and D. T. Blackstock (Acoustical Society of America, Melville, NY, 2008) Chap. 6, p. 177.
[7] E. H. Brandt, Acoustic physics: Suspended by sound, Nature **413**, 474 (2001).
[8] T. G. Leighton, A. J. Walton, and M. J. W. Pickworth, Primary Bjerknes forces, Eur. J. Phys. **11**, 47 (1990).
[9] See Supplemental Material at http://link.aps.org/supplemental/10.1103/PhysRevE.98.043103 for high-speed videos.
[10] U. Ingard, Acoustic wave generation and amplification in a plasma, Phys. Rev. **145**, 41 (1966).
[11] A. K. Mohanty and C. C. Oliver, Acoustic waves in pulsed microwave discharges, J. Phys. D **8**, 1202 (1975).
[12] V. A. Zhil'tsov, A. A. Skovoroda, and A. V. Timofeev, Spatially localized microwave discharge in the atmosphere as a source of sound, JETP **79**, 912 (1994).
[13] J. T. Dolan, M. G. Ury, and C. H. Wood, A novel high efficacy microwave powered light source, in *The Sixth International Symposium on the Science and Technology of Light Sources (Lighting Sciences 6)*, edited by L. Bartha and F. J. Kedves (Technical University of Budapest, 1992), pp. 301–302.
[14] J. T. Dolan, M. G. Ury, and C. H. Wood, Lamp including sulfur, U.S. Patent 5404076 A, Apr. 4, 1995.
[15] C. W. Johnston, H. W. P. van der Heijden, G. M. Janssen, J. van Dijk, and J. J. A. M. van der Mullen, A self-consistent

LTE model of a microwave-driven, high pressure sulfur lamp, J. Phys. D: Appl. Phys. **35**, 342 (2002).

[16] C. W. Johnston, H. W. P. van der Heijden, A. Hartgers, K. Garloff, J. van Dijk, and J. J. A. M. van der Mullen, An improved LTE model of a high pressure sulfur lamp, J. Phys. D: Appl. Phys. **37**, 211 (2004).

[17] S. Gavin, M. Carpita, and G. Courret, Power electronics for a sulfur plasma lamp working by acoustic resonance: Full scale prototype experimental results, in *Proceedings of the 16th European Conference on Power Electronics and Applications* (IEEE, Piscataway, NJ, 2014).

[18] G. Courret, P. Nikkola, S. Wasterlain, O. Gudozhnik, M. Girardin, J. Braun, S. Gavin, M. Croci, and P. W. Egolf, On the plasma confinement by acoustic resonance - An innovation for electrodeless high-pressure discharge lamps, Eur. Phys. J. D **71**, 214 (2017).

[19] J. P. Koulakis, A. L. F. Thornton, and S. Putterman, Magnetron coupling to sulfur plasma bulb, IEEE Trans. Plasma Sci. **45**, 2940 (2017).

[20] B. P. Turner, M. G. Ury, Y. Leng, and W. G. Love, Sulfur lamps. Progress in their development, J. Illum. Eng. Soc. **26**, 10 (1997).

[21] Diffusion of vorticity gives a few seconds as the time to spin up all the gas in the bulb.

[22] M. R. Moldover, M. Waxman, and M. Greenspan, Spherical acoustic resonators for temperature and thermophysical property measurements, High Temp. High-Pressures **11**, 75 (1979).

[23] J. P. Koulakis, S. Pree, and S. Putterman, Acoustic resonances in gas-filled spherical bulb with parabolic temperature profile (2018) (unpublished).

[24] J. P. Koulakis, S. Pree, A. L. F. Thornton, A. S. Nguyen, and S. Putterman, Pycnoclinic acoustic force, Proc. Meetings Acoust. **34**, 045005 (2018).

[25] G. Z. Gershuni and D. V. Lyubimov, *Thermal Vibrational Convection* (Wiley, New York, 1998).

[26] J. T. Karlsen, P. Augustsson, and H. Bruus, Acoustic Force Density Acting on Inhomogeneous Fluids in Acoustic Fields, Phys. Rev. Lett. **117**, 114504 (2016).

[27] L. D. Landau and E. M. Lifshitz, in *Course of Theoretical Physics: Fluid Mechanics*, 2nd ed. (Elsevier, Oxford, 1987), Chap. 76, p. 292.

[28] P. Collas and M. Barmatz, Acoustic radiation force on a particle in a temperature gradient, J. Acoust. Soc. Am. **81**, 1327 (1998).

[29] The rotation axis intersects the center of the bulb and is parallel to the direction of gravity.

[30] The emissivity of quartz at 1300 K was taken to be 0.65 ± 0.1 [46,47].

[31] K. T. Feldman, Review of the literature on Rijke thermoacoustic phenomena, J. Sound Vib. **7**, 83 (1968).

[32] K. T. Feldman, Review of the literature on Sondhauss thermoacoustic phenomena, J. Sound Vib. **7**, 71 (1968).

[33] M. Tanabe, T. Kuwahara, K. Satoh, T. Fujimori, J. Sato, and M. Kono, Droplet combustion in standing sound waves, Proc. Combust. Inst. **30**, 1957 (2005).

[34] T. Yano, K. Takahashi, T. Kuwahara, and M. Tanabe, Influence of acoustic perturbation and acoustically induced thermal convection on premixed flame propagation, Microgravity Sci. Technol. **22**, 155 (2010).

[35] R. Tuckermann, B. Neidhart, E. G. Lierke, and S. Bauerecker, Trapping of heavy gases in stationary ultrasonic fields, Chem. Phys. Lett. **363**, 349 (2002).

[36] G. W. Swift and S. Backhaus, The pulse tube and the pendulum, J. Acoust. Soc. Am. **126**, 2273 (2009).

[37] A. Swaminathan, S. L. Garrett, and R. W. Smith, Inhibition of Rayleigh-Benard convection through acceleration modulation for thermoacoustic devices, J. Acoust. Soc. Am. **141**, 3740 (2017).

[38] J. T. Karlsen and H. Bruus, Forces acting on a small particle in an acoustical field in a thermoviscous fluid, Phys. Rev. E **92**, 043010 (2015).

[39] J. T. Karlsen and H. Bruus, Acoustic Tweezing and Patterning of Concentration Fields in Microfluidics, Phys. Rev. Appl. **7**, 034017 (2017).

[40] R. Kippenhahn and A. Weigert, *Stellar Structure and Evolution* (Springer-Verlag, Berlin, 1990).

[41] D. Prialnik, *An Introduction to the Theory of Stellar Structure and Evolution*, 2nd ed. (Cambridge University Press, Cambridge, UK, 2009).

[42] S. A. Bludman and D. C. Kennedy, Analytic models for the mechanical structure of the solar core, Astrophys. J. **525**, 1024 (1999).

[43] P. Kervella, A. Mérand, and A. Gallenne, The circumstellar envelopes of the Cepheids ℓ Carinae and RS Puppis, Astron. Astrophys. **498**, 425 (2009).

[44] J. Davis, A. P. Jacob, J. G. Robertson, M. J. Ireland, J. R. North, W. J. Tango, and P. G. Tuthill, Observations of the pulsation of the Cepheid ℓ Car with the Sydney University stellar interferometer, Mon. Not. R. Astron. Soc. **394**, 1620 (2009).

[45] M. M. Taylor, M. D. Albrow, A. J. Booth, and P. L. Cottrell, The bright southern Cepheid ℓ Carinae: The radial velocity curve, distance and size, Mon. Not. R. Astron. Soc. **292**, 662 (1997).

[46] R. M. Sova, M. J. Linevsky, M. E. Thomas, and F. F. Mark, High-temperature infrared properties of sapphire, AlON, fused silica, yttria, and spinel, Infrared Phys. Technol. **39**, 251 (1998).

[47] J. R. Markham, P. R. Solomon, and P. E. Best, An FT-IR based instrument for measuring spectral emittance of material at high temperature, Rev. Sci. Instrum. **61**, 3700 (1998).